

## Digital Image Processing Techniques for Detection and Satellite Image Processing

Himadri Nath Moulick<sup>1</sup>, Moumita Ghosh<sup>2</sup>

<sup>1</sup>CSE, Aryabhata Institute of Engg & Management, Durgapur, PIN-713148, India

<sup>2</sup>CSE, University Institute Of Technology, (The University Of Burdwan) Pin -712104, India

**ABSTRACT:-** This paper describes the basic technological aspects of Digital Image Processing with special reference to satellite image processing. Basically, all satellite image-processing operations can be grouped into three categories: Image Rectification and Restoration, Enhancement and Information Extraction. The former deals with initial processing of raw image data to correct for geometric distortion, to calibrate the data radiometrically and to eliminate noise present in the data. The enhancement procedures are applied to image data in order to effectively display the data for subsequent visual interpretation. It involves techniques for increasing the visual distinction between features in a scene. The objective of the information extraction operations is to replace visual analysis of the image data with quantitative techniques for automating the identification of features in a scene. This involves the analysis of multispectral image data and the application of statistically based decision rules for determining the land cover identity of each pixel in an image. The intent of classification process is to categorize all pixels in a digital image into one of several land cover classes or themes. This classified data may be used to produce thematic maps of the land cover present in an image. Digital image processings of satellite data can be grouped into three categories : Image Rectification and Restoration, Enhancement and Information extraction. A digital remotely sensed image is composed of picture elements (pixels) located at the intersection of each row  $i$  and column  $j$  in each  $K$  bands of imagery. Each pixel is a number known as Digital Number (DN) or Brightness Value (BV).

**Keywords:-** defect detection, image processing, computer vision. Automated crack growth analysis, crack tip detection, digital image processing, double cantilever beam (DCB) fracture test, image filter, image subtraction.

### I. INTRODUCTION

Digital image processing technique is a great tool for improve the quality of image in different area. Image enhancement technique is a one of the preprocessing technique in digital image processing. Image enhancement technique is defined as a process of an image processing such that the result is much more suitable than the original image for a 'specific' application. This technique improve the quality of an image as perceived by a human. [7] It is a cosmetic procedure i.e. it does not add any extra information to the original image. It basically improve the subjective quality of the image by working with the existing data. For improving image quality more commonly used techniques are contrast stretch, density slicing, edge enhancement and spatial filtering. By using filtering technique we can remove various types of noise from the image [9]. Another technique in digital image processing is image segmentation which is use for extract the boundary of region. This process assists in detecting critical parts of the image that are not easily displayed in the original image. Noise can be remove by using clustering algorithms. The "Blind Source Separation" (BSS) problem of a vector of  $N$  mixtures  $X(\xi)$  created by  $M$  unknown sources  $S(\xi)$  by an  $N \times M$  sized mixing matrix  $A$  that is also unknown can be formulated by the equation:  $X(\xi) = AS(\xi) + N(\xi)$  [5]

### II. INDEPENDENT COMPONENT ANALYSIS (ICA)

One possible approach is to assume the independence of the sources with a method called Independent Component Analysis (ICA). Another assumption is the sources' sparsity assumption when there are properly represented according to a group of functions  $\{\phi_k(\xi)\}$ , meaning: [6]

$$s_m = \sum_k c_{mk} \phi_k(\xi) \quad (1)$$

The functions  $\phi_k(\xi)$  do not have to be linearly independent and can form an over complete set of functions like a Wavelets family. Assuming sparsity gives even better performance than standard ICA and even allows more sources than mixtures.

#### 1. ICA based Algorithms

ICA is presented in Three forms based on the coordinates. The first one integrates clustering and ICA algorithms and the other two are based only on ICA. For simplicity the algorithms are assumed with equal

number of mixtures and sources. [6] Thus the problem of estimating the number of sources is bypassed. However the ICA approach allows dealing with the case of the number of mixtures smaller than the number of sources also.

### 1.1 ICA Algorithm 1

This algorithm applies at the first stage the clustering algorithm. After this stage is finished, instead of separating the sources according to the centers of the clusters returned by the FCM algorithm, the unmixing matrix directly according to the Maximum Likelihood criterion is estimated, by finding the minimum of the function:

$$LW(Y) = k \cdot \ln(|\det W|) - \sum_{m=1..M} \sum_{k=1..K} v((WY)_{mk}) \tag{2}$$

This formula is received under the assumption of the independence of sources (the ICA assumption). The probability density function for the coefficients  $cmk$  is modeled as:  $p(cm_k) \propto \exp\{-v(cm_k)\}$  (3)

When  $v(x)$  is the absolute value function  $|x|$  with smoothing. The matrix  $Y$  appearing in the expression  $LW(Y)$  is the data matrix when in each row there are the DWP coefficients of one of the mixtures. In addition to that,  $k$  is the number of coefficients (called the number of features), and  $M=N$  is the number of sources and also the number of mixtures. The maximization of  $LW(Y)$  is performed effectively by the Natural Gradient algorithm. Using the estimated [4]  $W$  the sources are exactly reconstructed as in the case of square  $A$  in the clustering based algorithm.

### 1.2 ICA Algorithm 2

This algorithm starts with building the tree of DWP coefficients of mixtures exactly. After that a pass on all the subsets in the tree is performed and for each subset the following stages are performed:

1. Estimating the unmixing matrix  $W$  according to the ICA algorithm based on the current subset coefficients only.

2. After that the sources are reconstructed using the unmixing matrix of the previous stage. To these sources the DWP transform is applied, and their entropy is calculated in the Wavelet Transform domain. The entropy of a series of coefficients “coefficient” is:  $Entropy = \sum_{i=1..length(coeff)} [|\coeff[i]|]^{0.5}$  (4)

Normalizing the coefficients to have a square norm of 1:

$$[\sum_{i=1..LENGTH(COEFF)} |\text{COEFF}[i]|^2]^{0.5} = 1 \tag{5}$$

The entropy of the sources is calculated as the sum of entropies of each source separately. Finally, the “best” set as the set with the minimal entropy is chosen. This best set is chosen for reconstruction.

## III. CLUSTERING

Another approach to the sources separation, again under the assumption of sparsity is the clustering approach, to separate the coefficient data, generated after using a transform on the mixtures into several clusters where cluster is a group of condensed points. The data to separate will be collection of points of the form  $(d1k, d2k, \dots, dNk)$  when  $N$  is the number of mixtures and  $k$  runs on the indices of the family of functions  $\phi_k(\xi)$ . [2] for example in the simple case of two sources and two mixtures when the sources are already sparse in the original domain.

$$x1 = a11s1(t) + a12s2(t) \tag{6}$$

$$x2 = a21s1(t) + a22s2(t) \tag{7}$$

Since the sources are sparse in most cases when  $s1(t)$  is different than 0,  $s2(t)$  is equal to 0 and therefore:

$$x1 = a11s1(t)$$

$$x2 = a21s1(t) \tag{8}$$

Plotting the values of  $x1(t)$  v.s. the values of  $x2(t)$  will give straight line passing through the origin of the axes with a slope of  $a11/a21$ . Similarly when  $s2(t)$  is different from 0 and  $s1(t)$  is 0 (or close enough to 0) we get:

$$x1 = a12s2(t)$$

$$x2 = a22s2(t) \tag{9}$$

that in the same way is a description of a straight line passing through the origin of the axes with the slope of  $a12/a22$ . After finding the two slopes, we can reconstruct the mixing matrix  $A$  as it appears in the equation:

$$X = AS \tag{10}$$

When

$$X = (x_1(t) \ x_2(t))^T \tag{11}$$

and

$$S = (s_1(t) \ s_2(t))^T \tag{12}$$

assuming the mixing matrix is normalized, for example each column norm is 1.

As it turns out the sources are rarely sparse in their original domain, but their decomposition coefficients

according to a set of functions that is wisely chosen are usually sparse. Thus, the mixtures are not plotted by themselves, but the coefficients produced by a proper transform activated on them. [7] Also it is clear that the lines obtained, not always will be clear ones and therefore an algorithm is needed to estimate their slopes.

### 1. Clustering Based Algorithm

Before using this algorithm the Discrete Wavelet Packet (DWP) transform is applied to the mixtures received as input. As a result a tree of subsets of the transform coefficients is obtained. The following algorithm is applied to all the subsets of coefficients including the set of all the coefficients together.

#### 1.1 The Clustering Algorithm

1. All the coefficients of the subset for all the mixtures in the form of points in the mixtures space are taken and casted on the upper half of an N dimensional sphere with a radius of 1 (N is the number of mixtures).
2. The Fuzzy C-Means (FCM) clustering algorithm is executed on the resulting data with the number of clustering changing from 1 to a predefined maximum .
3. The output of the FCM algorithm is the centers of the clusters the data was separated.
4. Based on the clusters, centers from the previous stage optimal number of clusters are found and then the global distance measure for each subset are calculated: [6]  $\{GLOBAL\ DISTANCE\} = \{\sum ALL\ POINTS\ distance\ from\ center\ of\ point's\ cluster\} / \{num\ of\ points\}$  (13)

After those three stages is completed the “best set” is chosen according to minimum global distance. The assumption for the chosen set is that all the sources are “present” in it. For the chosen set the clusters’ centers are chosen and build from them the estimated mixing matrix when each center is one of its columns. Using that matrix the sources from mixtures are separated. In order to describe, the 2 cases are:

1. the number of mixtures is equal to the number of sources (n=m). the number of sources are estimated are exactly, therefore the estimated mixing matrix A is square. as stated before, the mixtures X for the noiseless case are given by:

$$X = AS \tag{14}$$

when s is the vector of sources, and so  $S = A^{-1}X = WX$  4.3

(W is called the unmixing matrix and the reconstruction of the sources is done the same way the construction of mixtures was done, but with the W matrix instead of A.)

2. The number of mixtures is different from the number of sources (N≠M). Here, assuming that the estimated number of sources are correct, A is not square (it is of size N\*M), and therefore, it has no inverse. The separation algorithm is: The chosen set (or sets) is taken and pass on all its clusters. For each cluster its coefficients are put into

the distinct set. The coefficients of the rest of the sets and the other clusters are zero. Finally, each source is reconstructed according to (the corresponding coefficients plugged into) the DWP tree. [5]

Description of the algorithm for estimating the number of clusters using the Hartman statistics:

For a collection of n points clustering is estimated to get k clusters C1, C2, ..., CK, when in each cluster  $N_R = |C_R|$  points ( $1 \leq R \leq K$ ).

$$D_R = \sum_{I, J \in C_R} (D_{IJ}) \tag{15}$$

when  $d_{ij}$  is the distance between points i and j (use the Euclidian distance  $\sum_k (X_{ik} - X_{jk})^2$  while k runs on all the dimensions of the points). Based on the  $D_r$  Parameter we define:

$$W(k) = \sum_{r=1..k} (1/2n_r) D_r \tag{16}$$

that is actually the sum of the average distances of the points from one another within each cluster on all the clusters.

The Hartigan statistics is then:

$$H(k) = [(W(k)/W(k+1))-1](n-k-1) \tag{17}$$

where k is the current number of clusters. H(k) for  $k = 1..MAX$  is calculated and choose the estimated number of clusters as the minimal k so that:

$$H(k) \leq TR \tag{18}$$

1.2 Results



Fig1: The Trained Output as a result of ICA Algorithm. – MIXING

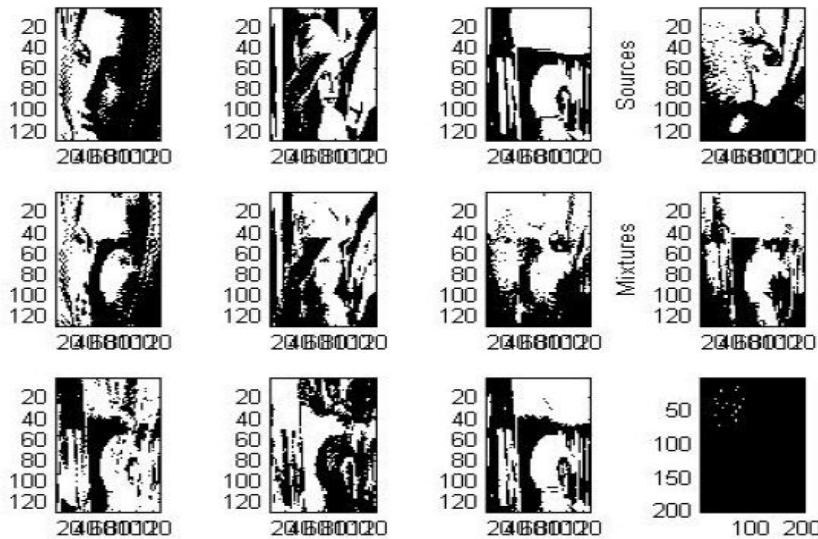


Fig2: The extract sources from the Unknown Sources as a Hartigan Product.

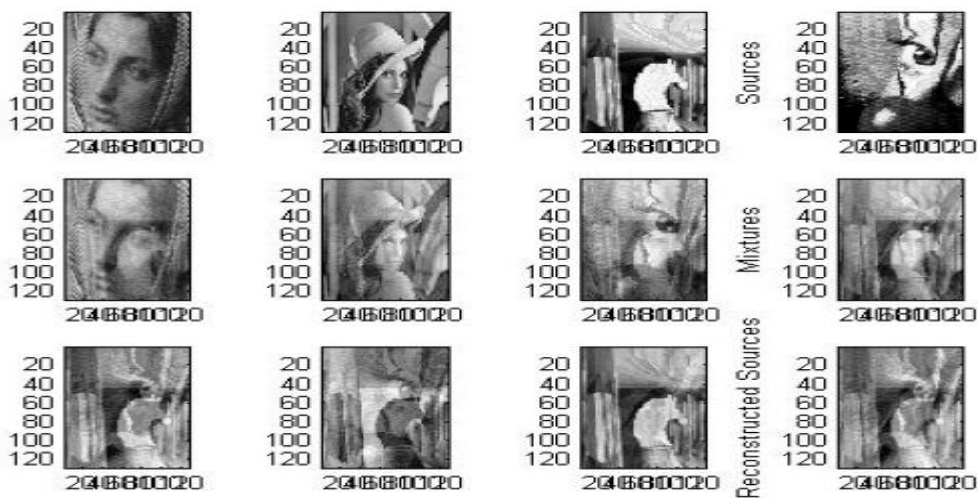
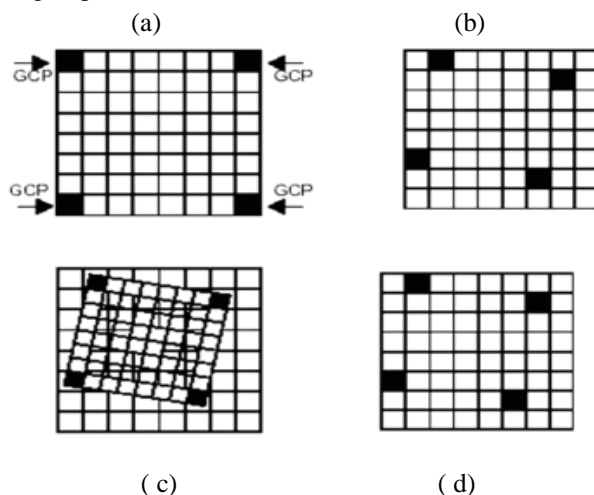


Fig3: Resultant images after removing Noise from the Images as a Restructured Result.

IV. SATELLITE IMAGE PROCESSING

A process by which an image is geometrically correcting is called Rectification . So, it is the process by which geometry of an image is made planimetric. Rectification is not necessary if there is no distortion in the

image. For example, if an image file is produced by scanning or digitizing a paper map that is in the desired projection system. Then that image is already planar and does not require rectification. Scanning and digitizing produce images that are planar. But it do not contain any map coordinate information. These images need only to be geo-referenced, which is a much simpler process than rectification. [10] Ground Control Points (GCP) are the specific pixels in the input image. For which the output map coordinates are known. To solve the transformation equations a least squares solution may be found that minimises the sum of the squares of the errors. when selecting ground control points as their number, quality and distribution affect the result of the rectification. The mapping transformation has been determined a procedure called resampling . Resampling matches the coordinates of image pixels to their real world coordinates . And then writes a new image on a pixel by pixel basis. Since the grid of pixels in the source image rarely matches the grid for the reference image. Using resampling method the output grid pixel values are calculated.

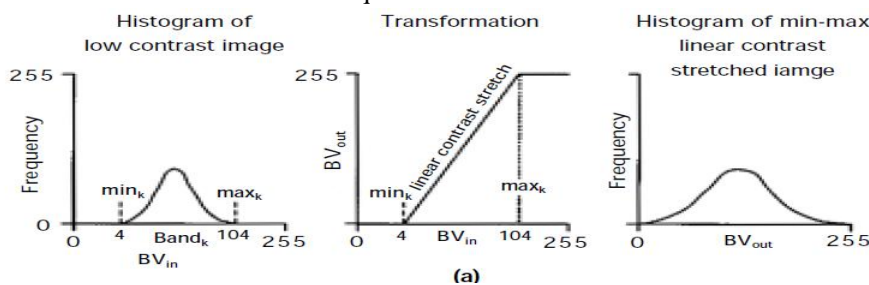


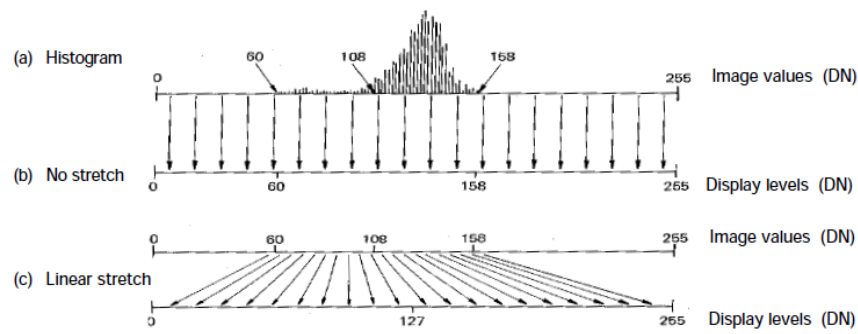
**Fig4:** Image Rectification (a & b) Input and reference image with GCP locations, (c) using polynomial equations the grids are fitted together, (d) using resampling method the output grid pixel values are assigned (source modified from ERDAS Field guide)

Image enhancement technique is defined as a process of an image processing such that the result is much more suitable than the original image for a ‘specific’ application. These techniques are most useful for many satellite images .A colour display give inadequate information for image interpretation. There exists a wide variety of techniques for improving image quality.[3] The contrast stretch, density slicing, edge enhancement, and spatial filtering are the more commonly used techniques. Image enhancement is used after the image is corrected for geometric and radiometric distortions. Image enhancement methods are applied separately to each band of a multispectral image. Contrast enhancement techniques expand the range of brightness values in an image. So that the image can be efficiently displayed in a desired manner by the analyst. Linear contrast stretch operation can be represented graphically as shown in Fig...The general form of the non-linear contrast enhancement is defined by

$$y = f(x) \quad (19)$$

Where x is the input data value and y is the output data value. The non-linear contrast enhancement techniques is useful for enhancing the colour contrast between the nearly classes and subclasses of a main class. Non linear contrast stretch involves scaling the input data logarithmically. Histogram equalization is another non-linear contrast enhancement technique.





**Fig5** : Linear Contrast Stretch (source Lillesand and Kiefer, 1993)

The three types of spatial filters used in remote sensor data processing are : Low pass filters, Band pass filters and High pass filters. The simple smoothing operation will blur the image, especially at the edges of objects. Blurring becomes more severe when the size of the kernel increases. Techniques that can be applied to deal with this problem include (i) by repeating the original border pixel brightness values ,artificially extending the original image beyond its border (ii) based on the image behaviour within a view pixels of the border, replicating the averaged brightness values near the borders. The most commonly used low pass filters are mean, median and mode filters. High-pass filtering is applied to remove the slowly varying components [1].And it enhance the high-frequency local variations.The high frequency filtered image will have a relatively narrow intensity histogram. The most valuable information that may be derived from an image is contained in the edges surrounding.The eyes see as pictorial edges are simply sharp changes in brightness value between two adjacent pixels. The edges may be enhanced using either linear or nonlinear edge enhancement techniques. In remotely sensed imagery ,a straight forward method of extracting edges is the application of a directional first-difference algorithm and approximates the first derivative between two adjacent pixels. Sometimes differences in brightness values from identical surface materials are caused by shadows, or seasonal changes in sunlight illumination angle and intensity. These conditions may hamper interpreter or classification algorithm to identify correctly surface materials or land use in a remotely sensed image. The mathematical expression of the ratio function is

$$BV_{i,j,r} = BV_{i,j,k} / BV_{i,j,l} \tag{20}$$

Where  $BV_{i,j,r}$  is the output ratio value for the pixel at row, i, column j;  $BV_{i,j,k}$  is the brightness value at the same location in band k, and  $BV_{i,j,l}$  is the brightness value in band l. Unfortunately, the computation is not always simple since  $BV_{i,j} = 0$  is possible. However, there are alternatives. For example, the mathematical domain of the function is  $1/255$  to  $255$  (i.e., the range of the ratio function includes all values beginning at  $1/255$ , passing through 0 and ending at 255). The way to overcome this problem is simply to give any  $BV_{i,j}$  with a value of 0 the value of 1. Ratio images can be meaningfully interpreted because they can be directly related to the spectral properties of materials .Figure 5 shows a situation where Deciduous and Coniferous Vegetation crops out on both the sunlit and shadowed sides of a ridge.

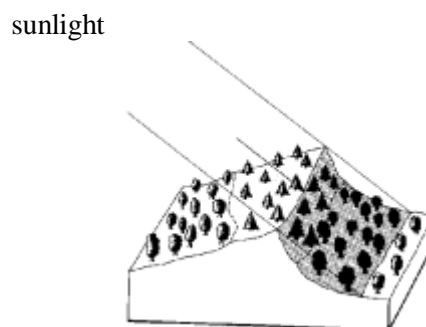


**Fig6** : Reduction of Scene Illumination effect through spectral ratioing (source Lillesand & Kiefer, 1993)

Most of sensors operate in two modes: *multispectral* mode and the *panchromatic* mode. The *panchromatic* mode corresponds [2] to the observation over a broad spectral band (similar to a typical black and white photograph) and the *multispectral* (color) mode corresponds to the observation in a number of relatively narrower bands. For example in the IRS – 1D, LISS III operates in the multispectral mode. Multispectral mode has a better spectral resolution than the panchromatic mode. Now coming to the spatial resolution, most of the satellites are such that the *panchromatic* mode has a better *spatial resolution* than the *multispectral* mode, for e.g. in IRS -1C, PAN has a spatial resolution of 5.8 m whereas in the case of LISS it is 23.5 m. The commonly applied Image Fusion Techniques are i) IHS Transformation ii). PCA iii). Brovey Transform iv). Band Substitution The traditional methods of classification mainly follow two approaches:

1. unsupervised : there are no specific algorithms. The unsupervised approach is referred to as clustering. A cluster is a collection of similar type of objects(data). The goal of clustering is to determine the intrinsic grouping in a set of unlabeled data. One common form of clustering, called the “K-means” clustering also called as ISODATA (Interaction Self-Organizing Data Analysis Technique).

2. Supervised: this have specific algorithms. The basic steps involved in a typical supervised classification procedure are 1. The training stage 2. Feature selection 3. Selection of appropriate classification algorithm 4. Post classification smoothening 5. Accuracy assessment

classification algorithms are the parallelepiped, minimum distance, and maximum likelihood decision rules. Parallelepiped algorithm is a widely used decision rule based on simple Boolean “and/or” logic. The parallelepiped algorithm is a computationally efficient method of classifying remote sensor data. Here requires training data. Minimum distance decision rule is computationally simple and commonly used. Like the parallelepiped algorithm, it also requires training data. It is possible to calculate this minimum distance using Euclidean distance based on the Pythagorean theorem. The maximum likelihood decision rule assigns each pixel having pattern measurements. It assumes that the training data statistics for each class in each band are normally distributed i.e Gaussian. Training data with bi-or trimodal histograms in a single band are not ideal. The Bayes’s decision rule is identical to the maximum likelihood decision rule that it does not assume that each class has equal probabilities. The maximum likelihood and Bayes’s classification require many more computations per pixel than either the parallelepiped or minimum-distance classification algorithms.

## V. CONCLUSION

For the case of mixtures without white noise the NSE and CTE measures are very much close and therefore they are practically the same measure of the quantity of separation, for the noised case there are larger differences between the two error, but still they are measure, but still they are close and the CTE is considered (cross talk error) as the error that shows us the separation quality when the nse is very much influenced by the noise energy. For the case of two non noised images none of the algorithms checked had problem to achieve visually good results in the sources separation. For the cases of three non noised images checked the best algorithm changed from clustering algorithm

for the first case of lena & woman & chess (error of 0.14-0.15%) to the 3rd ICA algorithm for the 2<sup>nd</sup> case of chess & woman & clown (error of 0.63-0.64%). in general the 1st and 3rd ICA algorithms have relatively good performance here while the 2nd ICA algorithm reaches pretty high errors (12% and 21- 22%) and also the clustering algorithm for the second case reaches the error of about 10%. for the case of two noised images the algorithm that achieves the lowest errors is undoubtedly the 3<sup>rd</sup> ICA algorithm with CTE of 0.25% and 0.001%. the other algorithms have much worse performance with relatively very high errors for the clustering algorithm and the 1st ICA algorithms for the case of lena & woman and better performance from them in the 2nd case of clown & chess (still highest error for the clustering algorithm). Digital image processings of satellite data can be primarily grouped into three categories : Image Rectification and Restoration, Enhancement and Information extraction. Image rectification is the pre-processing of satellite data for geometric and radiometric connections. Enhancement is applied to image data in order to effectively display data for subsequent visual interpretation. Information extraction is based on digital classification and is used for generating digital thematic map.

## REFERENCES

- [1]. Campbell, J.B. 1996. Introduction to Remote Sensing. Taylor & Francis, London. ERDAS IMAGINE 8.4 Field Guide: ERDAS Inc.
- [2]. Tomislav Petkovi cy, Josip Krapacz, Sven Lon cari cy. and Mladen Sercerz “Automated Visual Inspection of Plastic Products”.
- [3]. Walter Michaeli, Klaus Berdel “Inline-inspection-of-textured- plastics-surfaces” Optical Engineering 50(2),027205 (February 2011).

- [4]. K.N.Sivabalan , Dr.D.Ghanadurai (2010) “Detection of defects in digital texture images using segmentation”
- [5]. K.N.Sivabalan et. al. / International Journal of Engineering Science and Technology Vol. 2(10), 2010,
- [6]. Al-Omari A., Masad E. 2004. Three dimensional simulation of fluid flow in x-ray CT images of porous media. International Journal for Numerical and Analytical Methods in Geomechanics, 28, pp. 1327-1360.
- [7]. Alvarado C., Mahmoud E., Abdallah I., Masad E., Nazarian S., Langford R., Tandon V., Button J. 2007. Feasibility of quantifying the role of coarse aggregate strength on resistance to load in HMA. TxDOT Project No. 0-5268 and Research Report No. 0-5268.
- [8]. Banta L., Cheng K., Zaniewski J. 2003. Estimation of limestone particle mass from 2D images. Powder Technology, 132, 184 - 189.
- [9]. Chandan C., Sivakumar K., Masad E., Fletcher T. 2004. Application of imaging techniques to geometry analysis of aggregate particles. Journal of Computing in Civil Engineering, 18 (1), 75-82.
- [10]. T-W. Lee, M. Girolami, A.J. Bell, and T.J. Sejnowski, “A unifying information-theoretic framework for independent component analysis,” *International Journal on Mathematical and Computer Modeling*, in press, 1998.
- [11]. Bankman, I. (2000). *Handbook of Medical Imaging*, Academic Press, ISSN 0-12-077790-8, United States of America.
- [12]. Bidgood, D. & Horii, S. (1992). Introduction to the ACR-NEMA DICOM standard. *RadioGraphics*, Vol. 12, (May 1992), pp. (345-355)
- [13]. Jensen, J.R. 1996. Introduction to Digital Image Processing : A Remote Sensing Perspective. Practice Hall, New Jersey.
- [14]. Lillesand, T.M. and Kiefer, R. 1993. Remote Sensing Image Interpretation. John Wiley, New York.
- [15]. S. Amari, A. Cichocki, and H. H. Yang, “A new learning algorithm for blind signal separation,” *Advances in Neural Information Processing Systems*, vol. 8, pp. 752–763, 1996.
- [16]. A.J. Bell and T.J. Sejnowski, “An information-maximization approach to blind separation and blind deconvolution,” *Neural Computation*, vol. 7, pp. 1129–1159, 1995.
- [17]. T-W. Lee, M. Girolami, A.J. Bell, and T.J. Sejnowski, “A unifying information-theoretic framework for independent component analysis,” *International Journal on Mathematical and Computer Modeling*, in press, 1998.
- [18]. J.-F. Cardoso and B. Laheld, “Equivariant adaptive source separation,” *IEEE Trans. on Sig. Proc.*, vol. 44, no. 12, pp. 3017–3030, Dec. 1996.